Communications in Theoretical Physics

Leading Electroweak Corrections to the Neutral Higgs Boson Production at the Fermilab Tevatron*

Commun. Theor. Phys. (Beijing, China) **33** (2000) pp 275–284
© International Academic Publishers Vol. 33, No. 2, March 15, 2000

Leading Electroweak Corrections to the Neutral Higgs Boson Production at the Fermilab Tevatron*

CAO QingHong,[1] LI ChongSheng[1] and ZHU ShouHua[2,3]

[1]Department of Physics, Peking University, Beijing 100871, China

[2]CCAST (World Laboratory), P.O. Box 8730, Beijing 100080, China

[3]Institute of Theoretical Physics, Academia Sinica, P.O. Box 2735, Beijing 100080, China

(Received March 5, 1999)

Abstract *We calculate the leading electroweak corrections to the light neutral Higgs boson production via $q\bar{q}' \to WH$ at the Fermilab Tevatron in both the standard model and the minimal supersymmetric model, which arise from the top-quark and Higgs boson loop diagrams. We found that the leading electroweak corrections can exceed the QCD corrections for favorable values of the parameters in the MSSM, but such corrections are only about $-2\% \sim -4\%$ in the SM, which are much smaller than the QCD corrections. For the mass region of $90 < m_{h_0} < 120$ GeV, the leading electroweak corrections can reach -20% for large $\tan\beta$, and these corrections may be observable at a high luminosity Tevatron; at the least, new constraints on the $\tan\beta$ can be established.*

PACS numbers: 14.80.Bn, 14.80.Cp, 13.85.Qk, 12.60.Jv
Key words: electroweak correction, Higgs boson production

I. Introduction

One of the most important physics goals for future high energy physics is the discovery of Higgs boson. Recent direct search in the LEP2 experiments of running at $\sqrt{s} = 183$ GeV via the $e^+e^- \to Z^*H$ yields a lower bound of ~ 89.9 GeV on the Higgs mass.[1] Next year's running at 192 GeV will explore up to a Higgs boson mass of about 96 GeV.[2] After LEP2 the search for the Higgs particles will be continued at the CERN large hadron collider (LHC) for Higgs boson masses up to the theoretical upper limit. Before the LHC comes into operation it is worth while considering whether the Higgs boson can be discovered from the existing hadron collider, the Tevatron. Many investigations have been made in the detection of the Higgs boson at the Tevatron.[3] In Ref. [2], it was pointed out that if the Higgs boson is discovered at LEP2, it should be observed at the Tevatron's Run II with CM energy $\sqrt{s} = 2$ TeV and an integrated luminosity $\sim 10\,\mathrm{fb}^{-1}$, through the production subprocess $q\bar{q}' \to WH$, followed by $W \to \ell\bar{\nu}$ and $H \to b\bar{b}$; and if the Higgs boson lies beyond the reach of LEP2, $m_H \geq (95 \sim 100)$ GeV, then a $5-\sigma$ discovery will be possible in the above production subprocess in a future Run III with an integrated luminosity 30 fb^{-1} for masses up to $m_H \approx 125$ GeV. Since the expected number of events is small, it is important to calculate the cross section as accurate as possible. In Ref. [4] the $O(\alpha_s)$ QCD correction to the total cross section to this process has been calculated, and the QCD correction was found to be about 12% in the $\overline{\mathrm{MS}}$ scheme at the Fermilab Tevatron and the LHC in the standard model (SM). In general, the SM electroweak corrections are smaller comparing with the QCD correction. Beyond the SM, the electroweak corrections might be enhanced, since more Higgs bosons and the top quark with strong couplings are involved in the loop diagrams, for example, in the minimal supersymmetric model (MSSM),[5] which predict that the lightest Higgs boson h_0 is less than 140 GeV.[6] Therefore, it is worth while to calculate the electroweak corrections to the light Higgs boson production via $q\bar{q}' \to Wh_0$. In a previous paper[7] we calculated the $O(\alpha_{\mathrm{ew}} m_t^2/m_W^2)$ corrections arising from the top-quark loops to

*The project supported in part by National Natural Science Foundation of China, Doctoral Program Foundation of Higher Education, the Post Doctoral Foundation of China, and a grant from the State Commission of Science and Technology of China. ZHU ShouHua gratefully acknowledges the support of K.C. WONG Education Foundation, Hong Kong.

this process in both the SM and MSSM and found that in contrast to the QCD corrections which increase the tree-level cross sections, such corrections reduce the cross sections by about 2% $\sim$ 4% in the SM, and 2% $\sim$ 8% in the MSSM. However, in addition to these top-quark loop corrections, the Higgs boson loop corrections should also be taken into account, which are of order $Q(\alpha_{\rm ew}m_H^2/m_W^2)$; especially in the MSSM, such corrections may be comparable to the top-quark loop corrections, and even exceed them for large $\tan\beta$. In this paper, we consider the leading electroweak radiative corrections to the Higgs boson production at the Fermilab Tevatron in both the SM and MSSM. These corrections arise from the virtual effects of the third family (top and bottom) of quark, neutral and charged Higgs bosons, and neutral and charged Goldstone bosons. We present the corrections to production cross section versus Higgs boson mass changing in the region of 60 GeV $\leq m_{h_0} \leq$ 130 GeV for different values of $\tan\beta$, and compare with the results of the top-quark loops in the SM and MSSM, and also compare with the QCD corrections.

II. Calculations

The leading electroweak corrections to the process $q(p_1)\bar{q}'(p_2) \to W(k_1)h_0(k_2)$ arise from the Feynman diagrams shown in Figs 1 $\sim$ 4. We perform the calculation in the 't Hooft–Feynman gauge and use dimensional regularization to all the ultraviolet divergence in the virtual loop corrections utilizing the on-mass-shell renormalization,[8] in which the fine-structure constant α and the physical masses are chosen to be the renormalized parameters, and the finite parts of the counterterms are fixed by the renormalization conditions. As for the parameters β and α, for the MSSM we are considering, they have to be renormalized, too. In the MSSM they are not independent. Nevertheless, we follow the approach of Mendez and Pomarol[9] in which they considered them as independent renormalized parameters and fixed the corresponding renormalization constant by a renormalization condition that the on-mass-shell $H^+\bar{\ell}\nu_\ell$ and $h_0\bar{\ell}\ell$ couplings keep the forms of Eq. (3) of Ref. [9] to all orders of perturbation theory.

We define the Mandelstam variables as

$$\hat{s} = (p_1+p_2)^2 = (k_1+k_2)^2, \quad \hat{t} = (p_1-k_1)^2 = (p_2-k_2)^2, \quad \hat{u} = (p_1-k_2)^2 = (p_2-k_1)^2. \tag{1}$$

The relevant renormalization constants are defined as

$$m_{W0}^2 = m_W^2 + \delta m_W^2, \qquad m_{Z0}^2 = m_Z^2 + \delta m_Z^2, \tag{2}$$

$$\tan\beta_0 = (1+\delta Z_\beta)\tan\beta, \qquad \sin\alpha_0 = (1+\delta Z_\alpha)\sin\alpha, \tag{3}$$

$$W_0^{\pm\mu} = Z_W^{1/2}W^{\pm\mu} + \mathrm{i}Z_{H^\pm W}^{1/2}\partial^\mu H^\pm, \qquad H_0^\pm = (1+\delta Z_{H^\pm})^{1/2}H^\pm, \tag{4}$$

$$h_0 = (1+\delta h_0)^{1/2}h + Z_{h_0H}^{1/2}H, \qquad H_0 = (1+\delta Z_H)^{1/2}H + Z_{Hh_0}^{1/2}h. \tag{5}$$

Taking into account the leading electroweak corrections, the renormalized amplitude for $q\bar{q}' \to Wh_0$ can be written as

$$M_{\rm ren} = M_0 + \delta M^{\rm self} + \delta M^{\rm vertex}, \tag{6}$$

where M_0 is the amplitude at the tree level, $\delta M^{\rm self}$ and $\delta M^{\rm vertex}$ represent the corrections arising from the self-energy and vertex diagrams, respectively. M_0 is given by†

$$M_0 = \frac{e^2 m_W \sin(\beta-\alpha)}{\sqrt{2}(m_W^2-\hat{s})\sin^2\theta_W}\bar{d}(p_2)\not{\epsilon}P_L u(p_1), \tag{7}$$

where $P_{L,R} \equiv (1\mp\gamma_5)/2$. $\delta M^{\rm self}$ is given by

$$\delta M^{\rm self} = \frac{\delta m_W^2 + (m_W^2-\hat{s})\delta Z_W}{\hat{s}-m_W^2}M_0 + \delta M_t^{\rm self} + \delta M_H^{\rm self}, \tag{8}$$

$\delta M_t^{\rm self}$ represents the correction arising from the top-quark self-energy diagrams to the order $O(\alpha_{\rm ew}m_t^2/m_W^2)$, $\delta M_H^{\rm self}$ represents the corrections arising from the Higgs boson self-energy

†If we take the limit $m_{A_0} \to \infty$, then $\beta-\alpha \to \pi/2$ and both m_H and $m_{H^\pm} \to \infty$. As a result, m_{A_0}, m_H and $m_{H^\pm}$ decouple from the theory, and only m_{h_0} remains, the results come back to the case in SM.

diagrams to the order $O(\alpha_{ew} m_H^2/m_w^2)$, where $H = H^{\pm}, H, h, A_0$. The renormalization constant δm_w^2 and δZ_W are presented in the Appendix A. $\delta M_t^{\rm self}$ and $\delta M_H^{\rm self}$ are presented in the Appendix B.

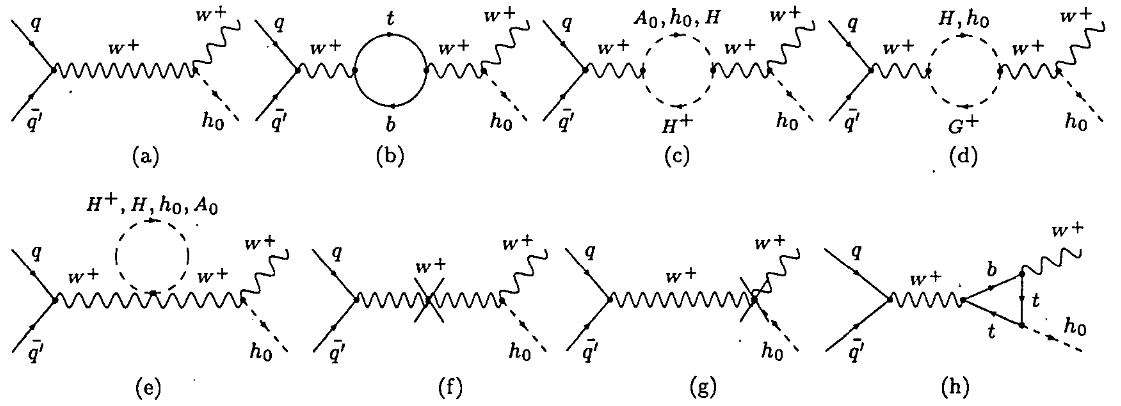

Fig. 1.

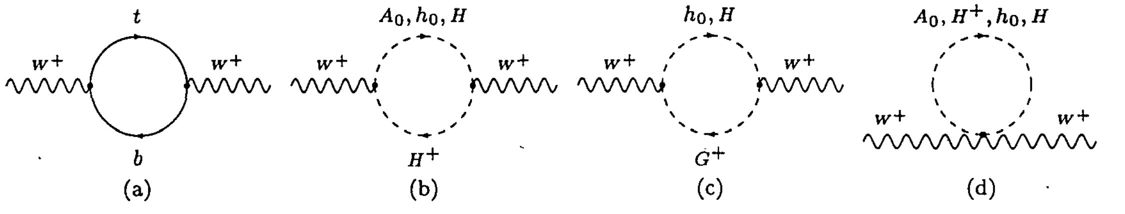

Fig. 2.

$\delta M^{\rm vertex}$ is given by

$$\delta M^{\rm vertex} = M_0\Big[\frac{1}{2}\delta Z_{h_0} + \frac{\delta m_w^2 - \delta m_z^2}{2(m_z^2 - m_w^2)} + \frac{\delta m_z^2}{m_z^2} + \frac{\delta m_w^2}{m_w^2} + \frac{\delta e}{e} + \cot(\beta-\alpha)(Z_{Hh_0}^{1/2} + \sin\beta\cos\beta\,\delta Z_\beta - \tan\alpha\,\delta Z_\alpha)\Big] + f_1^{\rm vertex}\bar{d}(p_2)\not\epsilon P_L u(p_1) + f_2^{\rm vertex}\bar{d}(p_2)\not p_1 P_L u(p_1)\epsilon\cdot p_1 + f_3^{\rm vertex}\bar{d}(p_2)\not p_1 P_L u(p_1)\epsilon\cdot p_2, \tag{9}$$

where

$$\delta Z_\beta = \frac{\delta m_z^2 - \delta m_w^2}{2(m_z^2 - m_w^2)} - \frac{\delta m_z^2}{2m_z^2} + \frac{\delta m_w^2}{2m_w^2} - \frac{1}{2}\delta Z_{H^\pm} - \frac{m_W}{\tan\beta} Z_{WH^\pm}^{1/2}, \tag{10}$$

$$\delta Z_\alpha = -\sin^2\beta\,\delta Z_\beta + \frac{\delta m_z^2 - \delta m_w^2}{2(m_z^2 - m_w^2)} - \frac{\delta m_z^2}{2m_z^2} + \frac{\delta m_w^2}{2m_w^2} - \frac{1}{2}\delta Z_{h_0} + \frac{\cos\alpha}{\sin\alpha} Z_{Hh_0}^{1/2}. \tag{11}$$

Note that $\delta e/e$ appearing in Eq. (9) contains no $O(\alpha m_t^2/m_w^2)$ nor $O(\alpha m_H^2/m_w^2)$ terms and does not need to be considered in our calculations. Although the renormalization constant $Z_{Hh_0}^{1/2}$ appears in δZ_α and the vertex counterterm, they cancel each other with accuracy and give no contribution to our calculation. Other renormalization constants are listed in the Appendix A and the vertex factors $f_{1,2,3}^{\rm vertex}$ are given in the Appendix C.

The corresponding amplitude squared for the process $q\bar{q}' \to Wh_0$ can be written as

$$\overline{\sum}|M_{\rm ren}|^2 = \overline{\sum}|M_0|^2 + 2{\rm Re}\overline{\sum}(\delta M^{\rm self} + \delta M^{\rm vertex})M_0^\dagger, \tag{12}$$

where the bar over the summation recalls average over initial parton spins. The cross section of process $q\bar{q}' \to Wh_0$ is

$$\hat{\sigma} = \int_{\hat{t}_{\rm min}}^{\hat{t}_{\rm max}} \frac{1}{16\pi\hat{s}^2}\overline{\sum_{\rm spins}}|M|^2\,{\rm d}\hat{t} \tag{13}$$

with

$$\hat{t}_{\min} = (m_{h_0}^2 + m_W^2 - \hat{s})/2 - \sqrt{(\hat{s} - (m_{h_0} + m_W)^2)(\hat{s} - (m_{h_0} - m_W)^2)}/2\,,$$
$$\hat{t}_{\max} = (m_{h_0}^2 + m_W^2 - \hat{s})/2 + \sqrt{(\hat{s} - (m_{h_0} + m_W)^2)(\hat{s} - (m_{h_0} - m_W)^2)}/2\,. \tag{14}$$

The total cross section of $P\bar{P} \to q\bar{q}' \to Wh_0$ can be obtained by folding the $\hat{\sigma}$ with the parton luminosity

$$\sigma(s) = \int_{(m_{h_0}+m_W)/\sqrt{s}}^{1} \mathrm{d}z \frac{\mathrm{d}L}{\mathrm{d}z} \hat{\sigma}(q\bar{q}' \to Wh_0 \text{ at } \hat{s} = z^2 s), \tag{15}$$

where $\sqrt{s}$ and $\sqrt{\hat{s}}$ are the CM energy of $P\bar{P}$ and $q\bar{q}'$, respectively, and $\mathrm{d}L/\mathrm{d}z$ is the parton luminosity, which is defined as

$$\frac{\mathrm{d}L}{\mathrm{d}z} = 2z \int_{z^2}^{1} \frac{\mathrm{d}x}{x} f_{q/P}(x, q^2) f_{q'/\bar{P}}(z^2/x, q^2), \tag{16}$$

where $f_{q/P}(x, q^2)$ and $f_{q'/\bar{P}}(z^2/x, q^2)$ are the parton distribution functions.[10]

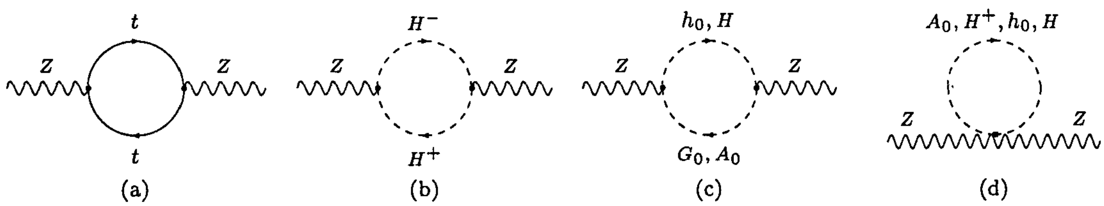

Fig. 3.

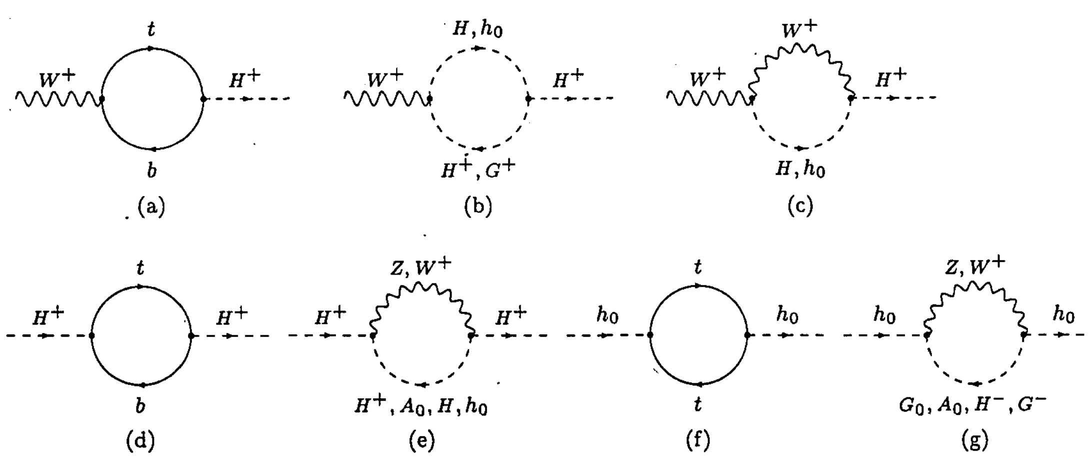

Fig. 4.

III. Numerical Results

In our numerical calculations, the SM parameters were taken to be $m_W = 80.33$ GeV, $m_Z = 91.187$ GeV, $m_t = 176$ GeV, $m_b = 4.5$ GeV and $\alpha_{\text{ew}} = 1/128$. Moreover, we use the relation[11] between the Higgs boson masses $m_{h_0,H,A,H^\pm}$ and parameters α, β at one-loop level, and choose m_{h_0} and $\tan\beta$ as two independent input parameters. As explained in Ref. [9], there is a small inconsistency in doing so since the parameters α and β of Ref. [6] are not the ones defined by the conditions given by Eq. (3) of Ref. [9]. Nevertheless, this difference would only induce a higher order change.[9] We will limit the value of $\tan\beta$ in the range $2 \leq \tan\beta \leq 30$, which is consistent with one required by the most popular MSSM model with scenarios motivated by current low energy data (including α_s, R_b and the branching ratio of $b \to s\gamma$).

In Figs 5 and 6 we present both the top-quark loop corrections[7] and the leading electroweak radiative corrections as functions of m_h for the different values of $\tan\beta$ using the CTEQ3L parton distributions for the tree-level cross sections σ_0 and the CTEQ3M parton distributions for the corrections $\delta\sigma$. From Fig. 5 one sees that the leading electroweak corrections are almost the same as the top-quark loop corrections in the SM, which means that the corrections arising from the Higgs boson loops are negligibly small in the SM. And these corrections are not sensitive to the mass of the Higgs boson and amount to $2\% \sim 4\%$ reduction in the tree-level total cross sections. However, in the MSSM, the Higgs boson loop corrections are important, and especially for large $\tan\beta\,(> 4)$, they can exceed the top-quark loop corrections. As a result, the leading electroweak corrections are much larger than the top-quark loop corrections. As shown in Fig. 6, for $\tan\beta = 30$, the leading electroweak corrections decrease the cross section by 70% when $m_h = 60$ GeV, while the top-quark loop corrections decrease only about -8%. However, these corrections are sensitive to m_{h_0}. For m_{h_0} in the range $90 \sim 120$ GeV, the leading electroweak corrections and the top-quark loop corrections drop to about $-20\% \sim -4\%$ and $-6\% \sim -2\%$, respectively, which indicate that the leading electroweak corrections are still obviously larger than those from the top-quark loops. Only in the vicinity of $m_{h_0} \approx 130$ GeV for all values of $\tan\beta$ the leading electroweak and top loop corrections are about the same as those in the SM.

Here, let us explain why the MSSM Higgs corrections become large for large $\tan\beta$. When $\tan\beta$ is large and m_{h_0} is small, $\beta - \alpha$ approaches π, and the tree-level cross sections are suppressed by the factor of $\sin^2(\beta - \alpha)$; however, radiative corrections contain terms such as $\cos(\alpha - \beta)$, which enhance the contributions from the corresponding terms, and the MSSM Higgs relative correction $\delta\sigma/\sigma_0$ becomes large.

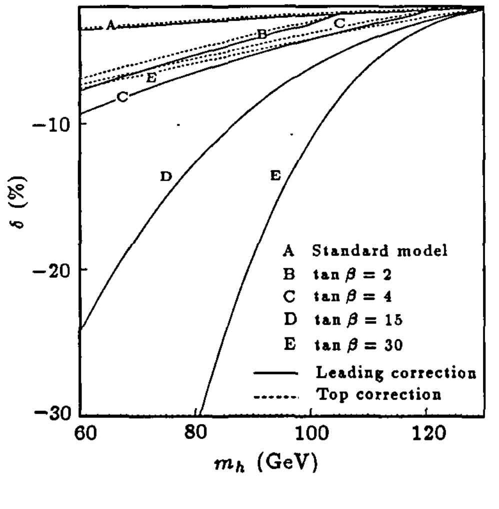

Fig. 5. Relative corrections $\delta\sigma/\sigma_0$ as functions of the Higgs boson mass of the process $q\bar{q}' \to Wh_0$ with $\sqrt{s} = 2$ TeV at Tevatron.

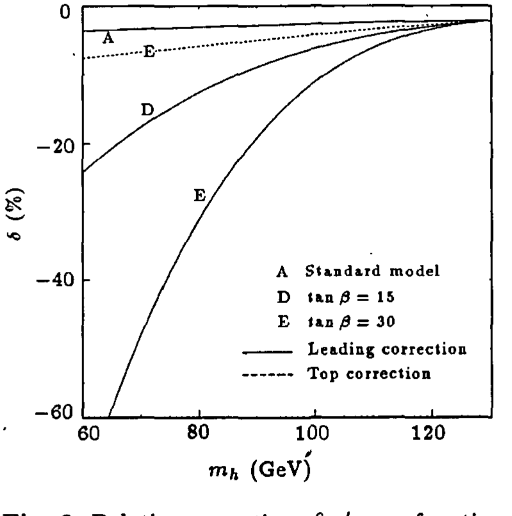

Fig. 6. Relative corrections $\delta\sigma/\sigma_0$ as functions of the Higgs boson mass of the process $q\bar{q}' \to Wh_0$ with $\sqrt{s} = 2$ TeV at Tevatron.

Comparing with the QCD corrections to this process,[4] which increase the tree-level total cross sections by about 12%, we find that in general the leading electroweak corrections partly cancel the QCD corrections; but for large $\tan\beta$, the magnitude of the former can even exceed the latter, and have to be considered in searching the light Higgs boson in the MSSM through this process at the Fermilab Tevatron.

To summarize, the leading electroweak radiative corrections, which combine the top-quark and the Higgs boson loop contributions, can exceed the QCD corrections for favorable values of the parameters in the MSSM, but such corrections are only about $-2\% \sim -4\%$ in the SM, which are much smaller than the QCD corrections. The mass region of $90 < m_{h_0} < 120$ GeV is the interesting window for searching the Higgs boson at the Tevatron, in which the leading electroweak corrections vary from -20% to -4% for $\tan\beta = 30$, and these corrections may be observable at a high luminosity Tevatron; at the least, new constraints on the $\tan\beta$ can be established.

Appendix A. The Renormalization Constants

$$\begin{aligned}
\delta m_W^2 = {} & \frac{N_c e^2 m_t^2}{96\pi^2 \sin^2\theta_W}\Big\{-2 + \frac{m_t^2}{m_W^2}[B_0(0,m_b^2,m_t^2) - B_0(m_W^2,m_b^2,m_t^2)] + 2B_0(0,m_b^2,m_t^2) \\
& - B_0(m_W^2,m_b^2,m_t^2) - 4B_0(0,m_t^2,m_t^2)\Big\} + \frac{e^2\sin^2(\beta-\alpha)}{192\pi^2\sin^2\theta_W}\Big\{-2m_H^2 - 4m_{H^+}^2 \\
& + \frac{m_H^4}{m_W^2}[B_0(m_W^2,m_H^2,m_{H^+}^2) - B_0(0,m_H^2,m_{H^+}^2)] + \frac{2m_H^2 m_{H^+}^2}{m_W^2}[B_0(0,m_H^2,m_{H^+}^2) \\
& - B_0(m_W^2,m_H^2,m_{H^+}^2)] + \frac{m_{H^+}^4}{m_W^2}[B_0(m_W^2,m_H^2,m_{H^+}^2) - B_0(0,m_H^2,m_{H^+}^2)] \\
& + m_H^2[-2B_0(m_W^2,m_H^2,m_{H^+}^2) - B_0(0,m_H^2,m_{H^+}^2)] + m_{H^+}^2[-2B_0(m_W^2,m_H^2,m_{H^+}^2) \\
& + B_0(0,m_H^2,m_{H^+}^2) - 2B_0(0,m_{H^+}^2,m_{H^+}^2)]\Big\} + \frac{e^2\cos^2(\beta-\alpha)}{192\pi^2\sin^2\theta_W}\Big\{-2m_{h_0}^2 - 4m_{H^+}^2 \\
& + \frac{m_{H^+}^4}{m_W^2}[B_0(m_W^2,m_{H^+}^2,m_{h_0}^2) - B_0(0,m_{H^+}^2,m_{h_0}^2)] + \frac{2m_{h_0}^2 m_{H^+}^2}{m_W^2}[B_0(0,m_{H^+}^2,m_{h_0}^2) \\
& - B_0(m_W^2,m_{H^+}^2,m_{h_0}^2)] + \frac{m_{h_0}^4}{m_W^2}[B_0(m_W^2,m_{H^+}^2,m_{h_0}^2) - B_0(0,m_{H^+}^2,m_{h_0}^2)] \\
& + m_{H^+}^2[-2B_0(m_W^2,m_{H^+}^2,m_{h_0}^2) - 2B_0(0,m_{H^+}^2,m_{H^+}^2) + B_0(0,m_{H^+}^2,m_{h_0}^2)] \\
& + m_{h_0}^2[-B_0(0,m_{H^+}^2,m_{h_0}^2) - 2B_0(m_W^2,m_{H^+}^2,m_{h_0}^2)]\Big\} + \frac{e^2}{192\pi^2\sin^2\theta_W}\Big\{-2m_{H^+}^2 \\
& - 4m_A^2 + \frac{m_A^4}{m_W^2}[B_0(m_W^2,m_A^2,m_{H^+}^2) - B_0(0,m_A^2,m_{H^+}^2)] \\
& + \frac{2m_A^2 m_{H^+}^2}{m_W^2}[B_0(0,m_A^2,m_{H^+}^2) - B_0(m_W^2,m_A^2,m_{H^+}^2)] + \frac{m_{H^+}^4}{m_W^2}[B_0(m_W^2,m_A^2,m_{H^+}^2) \\
& - B_0(0,m_A^2,m_{H^+}^2)] + m_A^2[-2B_0(m_W^2,m_A^2,m_{H^+}^2) - 2B_0(0,m_A^2,m_A^2) \\
& + B_0(0,m_A^2,m_{H^+}^2)] + m_{H^+}^2[-B_0(0,m_A^2,m_{H^+}^2) - 2B_0(m_W^2,m_A^2,m_{H^+}^2)]\Big\} \\
& + \frac{e^2\cos^2(\beta-\alpha)}{192\pi^2\sin^2\theta_W}\Big\{-4m_H^2 + \frac{m_H^4}{m_W^2}[B_0(m_W^2,m_H^2,m_W^2) - B_0(0,m_H^2,m_W^2)] \\
& + m_H^2[-4B_0(m_W^2,m_H^2,m_W^2) - 2B_0(0,m_H^2,m_H^2) + 3B_0(0,m_H^2,m_W^2)]\Big\} \\
& + \frac{e^2\sin^2(\beta-\alpha)}{192\pi^2\sin^2\theta_W}\Big\{-4m_{h_0}^2 + \frac{m_{h_0}^4}{m_W^2}[B_0(m_W^2,m_{h_0}^2,m_W^2) - B_0(0,m_{h_0}^2,m_W^2)] \\
& + m_{h_0}^2[-4B_0(m_W^2,m_{h_0}^2,m_W^2) - 2B_0(0,m_{h_0}^2,m_{h_0}^2) + 3B_0(0,m_{h_0}^2,m_W^2)]\Big\} \\
& + \frac{e^2 m_H^2}{64\pi^2\sin^2\theta_W}[1 + B_0(0,m_H^2,m_H^2)] + \frac{e^2 m_{H^+}^2}{32\pi^2\sin^2\theta_W}[1 + B_0(0,m_{H^+}^2,m_{H^+}^2)] \\
& + \frac{e^2 m_A^2}{64\pi^2\sin^2\theta_W}[1 + B_0(0,m_A^2,m_A^2)] + \frac{e^2 m_{h_0}^2}{64\pi^2\sin^2\theta_W}[1 + B_0(0,m_{h_0}^2,m_{h_0}^2)],
\end{aligned} \tag{A1}$$

$$
\begin{aligned}
\delta m_Z^2 = {} & \frac{N_C e^2 m_t^2}{288\cos^2\theta_W \pi^2 \sin^2\theta_W}[-18B_0(0,m_t^2,m_t^2) + 48\sin^2\theta_W B_0(0,m_t^2,m_t^2) \\
& - 64\sin^4\theta_W B_0(0,m_t^2,m_t^2) - 9B_0(m_Z^2,m_t^2,m_t^2) - 48\sin^2\theta_W B_0(m_Z^2,m_t^2,m_t^2) \\
& + 64\sin^2\theta_W B_0(0,m_t^2,m_t^2)] + \frac{e^2(\sin^2\theta_W - \cos^2\theta_W)^2}{96\cos^2\theta_W\pi^2\sin^2\theta_W}[-3m_{H^+}^2 - m_{H^+}^2 B_0(0,m_{H^+}^2,m_{H^+}^2) \\
& - 2m_{H^+}^2 B_0(m_Z^2,m_{H^+}^2,m_{H^+}^2)] + \frac{e^2\cos^2(\alpha-\beta)}{192\cos^2\theta_W\pi^2\sin^2\theta_W}\Big\{-2m_H^2 + \frac{m_H^4}{m_Z^2}[B_0(m_Z^2,m_H^2,m_Z^2) \\
& - B_0(0,m_H^2,m_Z^2)] + m_H^2[B_0(0,m_H^2,m_Z^2) - 4B_0(m_Z^2,m_H^2,m_Z^2)]\Big\} + \frac{e^2\sin^2(\alpha-\beta)}{192\cos^2\theta_W\pi^2\sin^2\theta_W} \\
& \times\Big\{-2m_H^2 - 4m_A^2 + \frac{(m_H^2-m_A^2)^2}{m_Z^2}[B_0(m_Z^2,m_A^2,m_H^2) - B_0(0,m_A^2,m_H^2)] \\
& + m_H^2[-B_0(0,m_A^2,m_H^2) - 2B_0(m_Z^2,m_A^2,m_H^2)] + m_A^2[-2B_0(m_Z^2,m_A^2,m_H^2) \\
& - 2B_0(0,m_A^2,m_A^2) + B_0(0,m_A^2,m_H^2)]\Big\} + \frac{e^2\sin^2(\alpha-\beta)}{192\cos^2\theta_W\pi^2\sin^2\theta_W}\Big\{-2m_{h_0}^2 \\
& + \frac{m_{h_0}^4}{m_Z^2}[B_0(m_Z^2,m_{h_0}^2,m_Z^2) - B_0(0,m_{h_0}^2,m_Z^2)] + m_{h_0}^2[B_0(0,m_{h_0}^2,m_Z^2) \\
& - 4B_0(m_Z^2,m_{h_0}^2,m_Z^2)]\Big\} + \frac{e^2\cos^2(\alpha-\beta)}{192\cos^2\theta_W\pi^2\sin^2\theta_W}\Big\{-2m_{h_0}^2 - 4m_A^2 \\
& + \frac{(m_{h_0}^2-m_A^2)^2}{m_Z^2}[B_0(m_Z^2,m_A^2,m_{h_0}^2) - B_0(0,m_A^2,m_{h_0}^2)] + m_{h_0}^2[-B_0(0,m_A^2,m_{h_0}^2) \\
& - 2B_0(m_Z^2,m_A^2,m_{h_0}^2)] + m_A^2[-2B_0(m_Z^2,m_A^2,m_{h_0}^2) - 2B_0(0,m_A^2,m_A^2) \\
& + B_0(0,m_A^2,m_{h_0}^2)]\Big\} + \frac{e^2(\sin^2\theta_W-\cos^2\theta_W)^2}{32\cos^2\theta_W\pi^2\sin^2\theta_W}m_{H^+}^2[1 + B_0(0,m_{H^+}^2,m_{H^+}^2)] \\
& + \frac{e^2}{64\cos^2\theta_W\pi^2\sin^2\theta_W}m_H^2[1 + B_0(0,m_H^2,m_H^2)] + \frac{e^2}{64\cos^2\theta_W\pi^2\sin^2\theta_W} \\
& \times m_{h_0}^2[1 + B_0(0,m_{h_0}^2,m_{h_0}^2)] + \frac{e^2}{64\cos^2\theta_W\pi^2\sin^2\theta_W}m_A^2[1 + B_0(0,m_A^2,m_A^2)]\,, \qquad \text{(A2)}
\end{aligned}
$$

$$
\begin{aligned}
\delta Z_W = {} & \frac{N_C e^2}{288\pi^2 m_W^4 \sin^2\theta_W}\{2m_W^4 - 6m_W^4 B_0(m_W^2,m_b^2,m_t^2) + 3m_t^4[B_0(m_W^2,m_b^2,m_t^2) \\
& - B_0(m_W^2,m_b^2,m_t^2)] + 3m_W^2(m_t^4 + m_t^2 m_W^2 - 2m_W^4)G_0(m_W^2,m_b^2,m_t^2)\} \\
& + \frac{e^2\sin^2(\beta-\alpha)}{576 m_W^4\pi^2\sin^2\theta_W}\{-2m_W^4 - 3m_W^4 B_0(m_W^2,m_H^2,m_{H^+}^2) + 3(m_H^2 - m_{H^+}^2)^2 \\
& \times[-B_0(0,m_H^2,m_{H^+}^2) + B_0(m_W^2,m_H^2,m_{H^+}^2)] + [6m_H^2 m_W^2 m_{H^+}^2 - 3m_H^4 m_W^2 \\
& - 3m_{H^+}^4 m_W^2 + 6m_H^2 m_W^4 + 6m_{H^+}^2 m_W^4 - 3m_W^6]G_0(m_W^2,m_H^2,m_{H^+}^2)\} \\
& + \frac{e^2\cos^2(\beta-\alpha)}{576 m_W^4\pi^2\sin^2\theta_W}\{-2m_W^4 - 3m_W^4 B_0(m_W^2,m_{H^+}^2,m_{h_0}^2) + 3(m_{h_0}^2 - m_{H^+}^2)^2 \\
& \times[B_0(m_W^2,m_{H^+}^2,m_{h_0}^2) - B_0(0,m_{H^+}^2,m_{h_0}^2)] + [6m_{h_0}^2 m_W^2 m_{H^+}^2 - 3m_{h_0}^4 m_W^2 \\
& - 3m_{H^+}^4 m_W^2 + 6m_{h_0}^2 m_W^4 + 6m_{H^+}^2 m_W^4 - 3m_W^6]G_0(m_W^2,m_{H^+}^2,m_{h_0}^2)\} \\
& + \frac{e^2}{576 m_W^4\pi^2\sin^2\theta_W}\{-2m_W^4 - 3m_W^4 B_0(m_W^2,m_A^2,m_{H^+}^2) + 3(m_A^2 - m_{H^+}^2)^2
\end{aligned}
$$

$$
\begin{aligned}
&\times [-B_0(0,m_A^2,m_{H^+}^2)+B_0(m_W^2,m_A^2,m_{H^+}^2)]+[6m_A^2m_W^2m_{H^+}^2-3m_A^4m_W^2\\
&-3m_{H^+}^4m_W^2+6m_A^2m_W^4+6m_{H^+}^2m_W^4-3m_W^6]G_0(m_W^2,m_A^2,m_{H^+}^2)\}\\
&+\frac{e^2\cos^2(\beta-\alpha)}{576m_W^4\pi^2\sin^2\theta_W}\{-2m_W^2-3m_W^4B_0(0,m_H^2,m_W^2)+3m_H^4[B_0(m_W^2,m_H^2,m_W^2)\\
&-B_0(0,m_H^2,m_W^2)]+6m_H^2m_W^2[B_0(0,m_H^2,m_W^2)-B_0(m_W^2,m_H^2,m_W^2)]\\
&+(12m_H^2m_W^4-3m_H^4m_W^2)G_0(m_W^2,m_H^2,m_W^2)\}+\frac{e^2\sin^2(\beta-\alpha)}{576m_W^4\pi^2\sin^2\theta_W}\{-2m_W^2\\
&-3m_W^4B_0(0,m_{h_0}^2,m_W^2)+3m_{h_0}^4[B_0(m_W^2,m_{h_0}^2,m_W^2)-B_0(0,m_{h_0}^2,m_W^2)]\\
&+6m_{h_0}^2m_W^2[B_0(0,m_{h_0}^2,m_W^2)-B_0(m_W^2,m_{h_0}^2,m_W^2)]\\
&+(12m_{h_0}^2m_W^4-3m_{h_0}^4m_W^2)G_0(m_W^2,m_{h_0}^2,m_W^2)\}\,, \qquad \text{(A3)}
\end{aligned}
$$

$$
\begin{aligned}
\delta Z_{H^\pm W}^{1/2}=&\frac{N_Ce^2m_t^2\cot\beta}{32m_{H^+}^2m_W^3\pi^2\sin^2\theta_W}\{m_t^2[B_0(0,m_b^2,m_t^2)-B_0(m_{H^+}^2,m_b^2,m_t^2)]\\
&+m_{H^+}^2B_0(m_{H^+}^2,m_b^2,m_t^2)\}-\frac{e^2\sin(\beta-\alpha)(m_{H^+}^2-m_H^2)}{64m_W^2m_{H^+}^2\pi^2\sin^2\theta_W\cos\theta_W}[2\cos\theta_Wm_W\cos(\alpha-\beta)\\
&-m_z\cos2\beta\cos(\alpha+\beta)][B_0(m_{H^+}^2,m_H^2,m_{H^+}^2)-B_0(0,m_H^2,m_{H^+}^2)]\\
&+\frac{e^2\sin(\beta+\alpha)(m_{h_0}^2-m_{H^+}^2)}{64m_W^2m_{H^+}^2\pi^2\sin^2\theta_W\cos\theta_W}[2\cos\theta_Wm_W\sin(\alpha-\beta)\\
&-m_z\cos2\beta\sin(\alpha+\beta)][B_0(m_{H^+}^2,m_{H^+}^2,m_{h_0}^2)-B_0(0,m_{H^+}^2,m_{h_0}^2)]\\
&+\frac{e^2\sin2\beta(m_H^2-m_W^2)}{64m_W^2m_{H^+}^2\pi^2\sin^2\theta_W\cos\theta_W}[\cos\theta_Wm_W\sin(\alpha-\beta)+m_z\cos(\beta+\alpha)\sin(2\beta)]\\
&\times[-B_0(m_{H^+}^2,m_H^2,m_W^2)+B_0(0,m_H^2,m_W^2)]+\frac{e^2\sin(\alpha-\beta)(m_{h_0}^2-m_W^2)}{64m_W^2m_{H^+}^2\pi^2\sin^2\theta_W\cos\theta_W}\\
&\times[-\cos\theta_Wm_W\cos(\alpha-\beta)+m_z\sin(\beta+\alpha)\sin(2\beta)][-B_0(m_{H^+}^2,m_{h_0}^2,m_W^2)\\
&+B_0(0,m_{h_0}^2,m_W^2)]+\frac{e^2\sin(\alpha-\beta)\cos(\alpha-\beta)}{64m_Wm_{H^+}^2\pi^2\sin^2\theta_W}\{m_H^2[B_0(0,m_H^2,m_W^2)\\
&-B_0(m_{H^+}^2,m_H^2,m_W^2)]-3m_{H^+}^2B_0(m_{H^+}^2,m_H^2,m_W^2)\}\\
&+\frac{e^2\sin(\alpha-\beta)\cos(\alpha-\beta)}{64m_Wm_{H^+}^2\pi^2\sin^2\theta_W}\{m_{h_0}^2[-B_0(0,m_{h_0}^2,m_W^2)+B_0(m_{H^+}^2,m_{h_0}^2,m_W^2)]\\
&+3m_{H^+}^2B_0(m_{H^+}^2,m_{h_0}^2,m_W^2)\}\,, \qquad \text{(A4)}
\end{aligned}
$$

$$
\begin{aligned}
\delta Z_{H^\pm}=&\frac{N_Ce^2m_t^2\cot^2\beta}{32m_W^2\pi^2\sin^2\theta_W}[-B_0(m_{H^+}^2,m_b^2,m_t^2)+(m_t^2-m_{H^+}^2)G_0(m_{H^+}^2,m_W^2,m_t^2)]\\
&+\frac{e^2(\sin^2\theta_W-\cos^2\theta_W)^2m_{H^+}^2}{16\pi^2\sin^2\theta_W\cos^2\theta_W}G_0(m_{H^+}^2,m_{H^+}^2,m_z^2)+\frac{e^2\sin(\alpha-\beta)^2(m_{H^+}^2+m_H^2)}{32\pi^2\sin^2\theta_W}\\
&\times G_0(m_{H^+}^2,m_H^2,m_W^2)+\frac{e^2\cos^2(\alpha-\beta)(m_{H_0}^2+m_{H^+}^2)}{32\pi^2\sin^2\theta_W}G_0(m_{H^+}^2,m_{H_0}^2,m_W^2)\\
&+\frac{e^2(m_{H^+}^2+m_A^2)}{32\pi^2\sin^2\theta_W}G_0(m_{H^+}^2,m_A^2,m_W^2)\,; \qquad \text{(A5)}
\end{aligned}
$$

$$
\delta Z_{h_0}=\frac{N_Ce^2m_t^2}{32m_W^2\pi^2}\cos^2\alpha\csc^2\beta[-B_0(m_{h_0}^2,m_t^2,m_t^2)+(4m_t^2-m_{h_0}^2)G_0(m_{h_0}^2,m_t^2,m_t^2)]
$$

$$+\frac{e^2\cos^2(\alpha-\beta)(m_{H^+}^2+m_{h_0}^2)}{16\pi^2\sin^2\theta_W}G_0(m_{h_0}^2,m_{H^+}^2,m_W^2)+\frac{e^2\sin^2(\alpha-\beta)m_{h_0}^2}{16\pi^2\sin^2\theta_W}$$
$$\times G_0(m_{h_0}^2,m_W^2,m_W^2)+\frac{e^2\sin^2(\alpha-\beta)m_{h_0}^2}{32\pi^2\sin^2\theta_W\cos^2\theta_W}G_0(m_{h_0}^2,m_Z^2,m_Z^2)$$
$$+\frac{e^2\cos^2(\alpha-\beta)(m_A^2+m_{h_0}^2)}{32\pi^2\sin^2\theta_W\cos^2\theta_W}G_0(m_{h_0}^2,m_A^2,m_Z^2)\,; \tag{A6}$$

Here and below, B_0, C_0, C_i and C_{ij} is the two-point and three-point scalar integrals, the definitions for them can be found in Ref. [12] and G_0 is the derivative of B_0 which is expressed as $G_0(M^2,m_1^2,m_2^2)=\partial B_0(k^2,m_1^2,m_2^2)/\partial k^2|_{k^2=M^2}$.

Appendix B. Self-Energy Corrections

$$\delta M_T^{\rm self}=\frac{N_c e^4 m_W\sin(\beta-\alpha)}{288\sqrt{2}\pi^2\hat{s}(-m_W^2+\hat{s})^2\sin^4\theta_W}[6\hat{s}m_t^2-2\hat{s}^2+3m_t^2(m_t^2-2\hat{s})$$
$$\times B_0(0,m_b^2,m_t^2)+3(-m_t^4-\hat{s}m_t^2+2\hat{s}^2)B_0(\hat{s},m_b^2,m_t^2)]\,, \tag{B1}$$

$$\delta M_H^{\rm self}=-\frac{e^4 m_W\sin^3(\beta-\alpha)}{64\sqrt{2}\pi^2(m_W^2-\hat{s})^2\sin^4\theta_W}\Big[\frac{2}{9}(3m_H^2-6m_{H^+}^2-\hat{s})+\frac{2m_{H^+}^2}{3}B_0(0,m_{H^+}^2,m_{H^+}^2)$$
$$+\frac{(m_{H^+}^2-m_H^2)(m_{H^+}^2-m_H^2-\hat{s})}{3\hat{s}}B_0(0,m_H^2,m_{H^+}^2)$$
$$+\frac{[(m_{H^+}-m_H)^2-\hat{s}][\hat{s}-(m_{H^+}+m_H)^2]}{3\hat{s}}B_0(\hat{s},m_H,m_{H^+}^2)\Big]$$
$$-\frac{e^4 m_W\cos^2(\beta-\alpha)\sin(\beta-\alpha)}{64\sqrt{2}\pi^2(m_W^2-\hat{s})^2\sin^4\theta_W}\Big\{\frac{2}{9}(3m_{h_0}^2+6m_{H^+}^2-\hat{s})+\frac{2m_{H^+}^2}{3}B_0(0,m_{H^+}^2,m_{H^+}^2)$$
$$+\frac{(m_{H^+}^2-m_{h_0}^2)(m_{H^+}^2-m_{h_0}^2-\hat{s})}{3\hat{s}}B_0(0,m_{H^+}^2,m_{h_0}^2)$$
$$+\frac{[(m_{H^+}-m_{h_0})^2-\hat{s}][\hat{s}-(m_{H^+}+m_{h_0})^2]}{3\hat{s}}B_0(\hat{s},m_{H^+}^2,m_{h_0}^2)\Big\}$$
$$+\frac{e^4 m_W\sin(\beta-\alpha)}{64\sqrt{2}\pi^2(m_W^2-\hat{s})^2\sin^4\theta_W}\Big\{\frac{2}{9}(6m_A^2+3m_{H^+}^2-\hat{s})+\frac{2m_A^2}{3}B_0(0,m_A^2,m_A^2)$$
$$+\frac{(m_{H^+}^2-m_A^2)(m_{H^+}^2-m_A^2-\hat{s})}{3\hat{s}}B_0(0,m_A^2,m_{H^+}^2)$$
$$+\frac{[(m_{H^+}-m_A)^2-\hat{s}][\hat{s}-(m_{H^+}+m_A)^2]}{3\hat{s}}B_0(\hat{s},m_A,m_{H^+}^2)\Big\}$$
$$-\frac{e^4 m_W\sin(\beta-\alpha)\cos^2(\beta-\alpha)}{64\sqrt{2}\pi^2(m_W^2-\hat{s})^2\sin^4\theta_W}\Big\{\frac{2}{9}(6m_H^2-\hat{s})+\frac{2m_H^2}{3}B_0(0,m_H^2,m_H^2)$$
$$+\Big[\frac{(m_H^2-m_W^2)(m_H^2-m_W^2-\hat{s})}{3\hat{s}}-\frac{m_W^2}{3}\Big]B_0(0,m_H^2,m_W^2)$$
$$+\Big[\frac{[(m_H-m_W)^2-\hat{s}][\hat{s}-(m_H+m_W)^2]}{3\hat{s}}-\frac{2m_W^2}{3}\Big]B_0(\hat{s},m_H^2,m_W^2)\Big\}$$
$$-\frac{e^4 m_W\sin(\beta-\alpha)^3}{64\sqrt{2}\pi^2(m_W^2-\hat{s})^2\sin^4\theta_W}\Big\{\frac{2}{9}(6m_{h_0}^2-\hat{s})+\frac{2m_{h_0}^2}{3}B_0(0,m_{h_0}^2,m_{h_0}^2)$$
$$+\Big[\frac{(m_{h_0}^2-m_W^2)(m_{h_0}^2-m_W^2-\hat{s})}{3\hat{s}}-\frac{m_W^2}{3}\Big]B_0(0,m_{h_0}^2,m_W^2)$$
$$+\Big[\frac{[(m_{h_0}-m_W)^2-\hat{s}][\hat{s}-(m_{h_0}+m_W)^2]}{3\hat{s}}-\frac{2m_W^2}{3}\Big]B_0(\hat{s},m_{h_0}^2,m_W^2)\Big\}$$

$$
\begin{aligned}
&+\frac{e^4 m_W \sin(\beta-\alpha) m_H^2}{64\sqrt{2}\pi^2 (m_W^2-\hat{s})^2 \sin^4\theta_W}[1+B_0(0,m_H^2,m_H^2)]+\frac{e^4 m_W \sin(\beta-\alpha) m_{H^+}^2}{64\sqrt{2}\pi^2 (m_W^2-\hat{s})^2 \sin^4\theta_W}\\
&\times[1+B_0(0,m_{H^+}^2,m_{H^+}^2)]+\frac{e^4 m_W \sin(\beta-\alpha) m_{h_0}^2}{64\sqrt{2}\pi^2 (m_W^2-\hat{s})^2 \sin^4\theta_W}[1+B_0(0,m_{h_0}^2,m_{h_0}^2)]\\
&+\frac{e^4 m_W \sin(\beta-\alpha) m_A^2}{64\sqrt{2}\pi^2 (m_W^2-\hat{s})^2 \sin^4\theta_W}[1+B_0(0,m_A^2,m_A^2)]\,.
\end{aligned}
\tag{B2}
$$

Appendix C. The Vertex Form Factors

$$
\begin{aligned}
f_1^{\text{vertex}} =& \frac{-N_c e^4 m_t^2}{32\sqrt{2}\, m_W\, \pi^2\,(m_W^2-\hat{s})\sin^4\theta_W}[-2B_0(\hat{s},m_b^2,m_t^2)+(-2m_t^2-\hat{t})\\
&\times C_0(m_{h_0}^2,m_W^2,\hat{s},m_t^2,m_t^2,m_b^2)+(-2m_W^2-\hat{t})C_1(m_W^2,\hat{s},m_{h_0}^2,m_t^2,m_b^2,m_t^2)\\
&+(-m_{h_0}^2-2\hat{t})C_2(m_W^2,\hat{s},m_{h_0}^2,m_t^2,m_b^2,m_t^2)\\
&+4C_{00}(m_W^2,\hat{s},m_{h_0}^2,m_t^2,m_b^2,m_t^2)]\,,
\end{aligned}
\tag{C1}
$$

$$
\begin{aligned}
f_2^{\text{vertex}} =& \frac{-N_c\, e^4 m_t^2}{16\sqrt{2}\, m_W\, \pi^2\,(m_W^2-\hat{s})\,\sin^4\theta_W}[-C_0(m_{h_0}^2,m_W^2,\hat{s},m_t^2,m_t^2,m_b^2)\\
&-C_1(m_W^2,\hat{s},m_{h_0}^2,m_t^2,m_b^2,m_t^2)-3C_2(m_W^2,\hat{s},m_{h_0}^2,m_t^2,m_b^2,m_t^2)\\
&-2C_{12}(m_W^2,\hat{s},m_{h_0}^2,m_t^2,m_b^2,m_t^2)-2C_{22}(m_W^2,\hat{s},m_{h_0}^2,m_t^2,m_b^2,m_t^2)]\,,
\end{aligned}
\tag{C2}
$$

$$
\begin{aligned}
f_3^{\text{vertex}} =& \frac{-N_c e^4 m_t^2}{16\sqrt{2}\, m_W\, \pi^2\,(m_W^2-\hat{s})\,\sin^4\theta_W}[-C_2(m_W^2,\hat{s},m_{h_0}^2,m_t^2,m_b^2,m_t^2)\\
&-2C_{12}(m_W^2,\hat{s},m_{h_0}^2,m_t^2,m_b^2,m_t^2)-2C_{22}(m_W^2,\hat{s},m_{h_0}^2,m_t^2,m_b^2,m_t^2)]\,.
\end{aligned}
\tag{C3}
$$

References

[1] P. McNamara, *ICHEP '98*, Vancouver, July (1998).

[2] C. Quigg, Fermilab-conf-98/059-T, hep-ph/9802320.

[3] A. Stange, W. Marciano and S. Willenbrock, Phys. Rev. **D49** (1994) 1354; ibid. **D50** (1994) 4491; S. Kim, S. Kuhlman and W. Yao, cdf-anal-exotic-public-3904, Oct. (1996); W. Yao, Fermilab-conf-96-383-E, Jun. (1996); J. Womersley, D0 Note 3227, Apr. (1997); S. Parke, Fermilab-conf-97/335-T.

[4] T. Han and S. Willenbrock, Phys. Lett. **B273** (1990) 167; J. Ohnemus and W.J. Stirling, Phys. Rev. **D47** (1993) 2722; H. Baer, B. Bailay and J.F. Owens, Phys. Rev. **D47** (1993) 2730; S. Smith and S. Willenbrock, Phys. Rev. **D54** (1996) 6696.

[5] H.E. Haber and G.L. Kane, Phys. Rep. **117** (1985) 75; J.F. Gunion and H.E. Haber, Nucl. Phys. **B272** (1986) 1.

[6] J. Gunion and A. Turski, Phys. Rev. **D39** (1989) 2701; ibid. **D40** (1990) 2333; J.R. Espinosa and M. Quiros, Phys. Lett. **B266** (1991) 389; M. Carena, M. Quiros and C.E.M. Wagner, Nucl. Phys. **B461** (1996) 407.

[7] C.S. LI and S.H. ZHU, Phys. Lett. **B444** (1998) 224.

[8] S. Sirlin, Phys. Rev. **D22** (1980) 971; W.J. Marciano and A. Sirlin, ibid. **D22** (1980) 2695; ibid. **D31** (1985) 213; A. Sirlin and W.J. Marciano, Nucl. Phys. **B189** (1981) 442; K.I. Aoki *et al.*, Prog. Theor. Phys. Suppl. **73** (1982) 1.

[9] A. Mendez and A. Pomarol, Phys. Lett. **B279** (1992) 98.

[10] H.L. Lai, J. Botts, J. Huston, *et al.*, Phys. Rev. **D51** (1995) 4763.

[11] M. Spiral, CERN-th/97-68 (hep-ph/9705337).

[12] G. Passarino and M. Veltman, Nucl. Phys. **B33** (1979) 151; A. Denner, Fortschr. Phys. **41** (1993) 4.